Microstructural Characterization and Mechanical Properties of Rapidly Solidified Al-Si Systems by Chill Block Melt-Spinning Technique.

DOI: https://doi.org/10.24297/jap.v17i.8607

Rizk Mostafa Shalaby[1], Amal Abdallah[1], Mustafa Kamal[1]

[1]Metal Physics Laboratory, Physics Department, Faculty of Science, Mansoura University, Mansoura, Egypt.

amal.elsherif11@gmail.com, rizk2002@mans.edu.eg

Abstract

ALSi alloys with compositions (0, 0.1, 0.5, 0.9, and 1.3 wt.% Si) were manufactured by chill block melt spinning method. The resulting ribbons samples have been characterized by x-ray diffraction (XRD) and scanning electron microscope (SEM). Detailed analysis of (XRD) shows that presence of f.c.c Al solid solution and Si particles embedded within the aluminum grains. The microstructural examination resulted that the microstructure of the melt-spun ribbons is finer and uniformly distributed. Rapid solidification technology led to increase the solubility of Si in α-Al as confirmed by XRD. Micro hardness measurements were also carried out by Vickers micro-hardness tester at applied load 25gm forced and different dwell time. It is concluded that the Vickers hardness values are sensitive to applied load and indentation time. It is also found that the highest values of Hv is sensitive to presence of Si as columnar shape with fine-grained of Al by high cooling rate.

Keywords: ALSi Alloys, Structure, Microstructure, Mechanical Properties, Micro Hardness Test, Electrical Resistivity, Micro-Creep

1. Introductions

Aluminum-Silicon alloys are used on a large scale in different fields of industry. These alloys are multipurpose matter, it comprises a large present of the total cast parts of aluminum reach to 85% to 90% produced for aerospace and automotive field industry[1,2]. Aluminum-silicon alloys where Al is a base element in alloying, include a type of material, which enhance the most important part of all shaped castings that used in manufacture, these alloys have a lot of applications in the aerospace and automotive industries [3]. This is because of the effect of silicon that affect effectively in the enhancement of casting features, in addition to other physical properties, like corrosion resistance and mechanical properties [4]. These alloys also used heavily in buildings fields and constructions, packaging marine, containers, aviation, aerospace, and electrical industries due to their features as corrosion resistance and lightweight, in most environments. Mechanical properties are controlled by the Manipulation in the microstructure through adding small alloying elements. During solidification, microstructure evolution of hypoeutectic Al-Si alloys is in two periods: primary dendrite AL phase formation (α-matrix), and subsequently eutectic transformation (eutectic Si particles in α-matrix). Depending on the distribution and the shape of the silicon particles ,the mechanical properties of Al-Si alloys are determined [5]. Nowadays Aluminum alloys or other lightweight alloys have a lot of application in manufacturing industries and automotive industries, as they augment the engine efficiency because they have the ability to reduce weight along with it can retain the strength that is desired to resist the same strength of cast iron. These lightweight alloys also decrease the consumption of shields the surroundings and fuel, so steel parts and cast iron can replaced by it successfully[6–8]. The development of aluminum base alloys which have important features such as low weight, high stiffness and high tensile strength have extensively been required because of its expectation of the improvement of structural efficiency to reduce fuel consumption and transportation vehicle. Although there are a lot of materials are used in rapid solidification technique, Al-Si alloys are very favored because of Si has a very limited solid solubility in Al in conventional techniques[9,10]. Based on Si concentration in weight percent (wt.%), the system of Al-Si alloy located in three stages: hypoeutectic area (<12% Si), eutectic area (12-13% Si) and hypereutectic as seen in the equilibrium phase diagram (Fig. 1)[11]. The aluminum density is 2.7, besides that, the low density of Silicon (2.34 g cm^{-3}) is a very important property, this advantage is used to

reduce the overall weight of the cast component. Although the solubility of silicon in aluminum is very low, silicon is deposited almost pure, which is hard and thus promotes corrosion resistance [12]. Si decrease the melting temperature, rises the melt fluidity, decreases the contraction associated with solidification and the raw material of silicon is very cheap. Besides, the comparatively low thermal expansion coefficient, high fluidity and wear resistance that are a very important properties of Al_Si alloys that gave it wide attention in this alloy family and preferred it in aerospace and automotive applications [7,12]. Applying different rapid solidification techniques became on wide range of composition of AL_Si alloys as compared to conventionally processes because the recent results have pretended that this processes may elementally modify the morphology of the Silicon phase. (RSP) Rapid solidification technique at cooling rates more than 10^3 K/s allows us to prepare alloys with extraordinary properties; i.e. extended solid solution ranges, reduction in grain sizes, decreased the levels of segregation and gave the formation of metastable phases in some cases. Utilizing the chill-block melt-spun technique of rapid quench from the liquid, a number of alloy systems have been investigated in search of extended terminally solubility ranges or metastable intermediate phases. Applying Melt spinning technique with cooling rates more than 106 K/s produce ribbons have mechanical and thermal properties better than other conventionally processes [10,13][10].In this work, the ALSi binary systems has been chosen essentially because of its industrial importance. So, the present work aimed to study of microstructural characterization and mechanical properties of melt_spun AL_Si binary alloys.

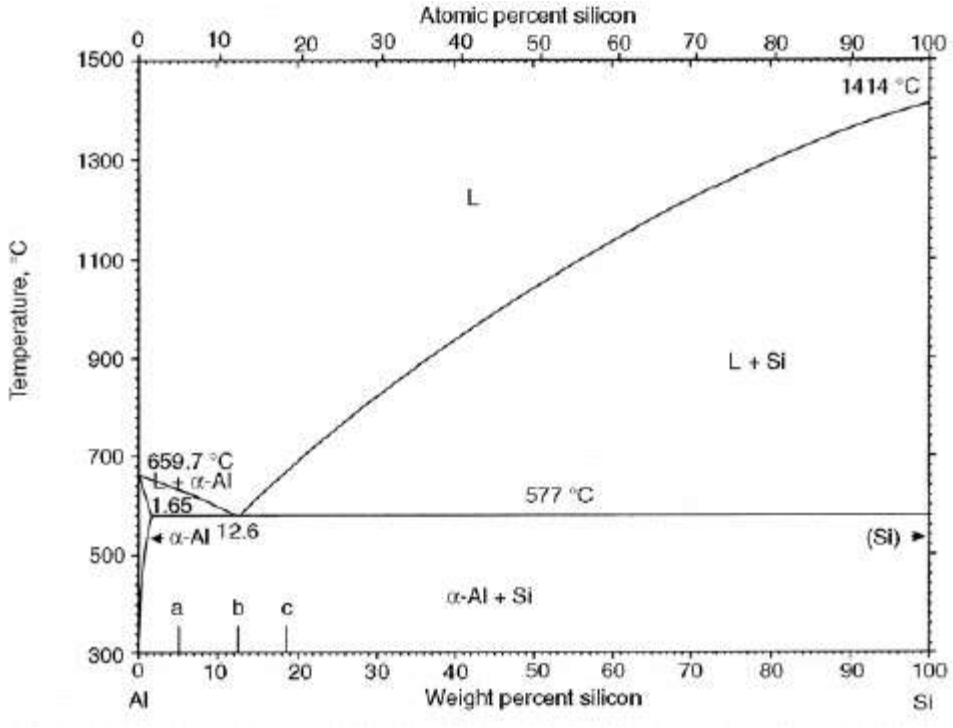

Fig.1: Phase equilibrium diagram of Al-Si alloy[11].

2. Experimental procedures

AL_Si alloys were prepared at different contents of Si by utilizing melting commercially pure Al (99.95%) and commercially pure Si (99.95%) in a crucible from graphite at high-frequency induction furnace, and the melt was held at 750 °C to achieve homogeneous mix. In this work, we prepared 5 alloys of Al_Si have compositions Al pure, AL_1Si%, AL_5Si%, AL_9Si% and AL_13 Si%, forms ribbons have thickness about rang 0.012-0.018 cm and width from rang 0.40-0.50cm. were produced by melt_spinning technique via a single copper roller [14], that supposed that the ribbons got, are completely solid at a distance "d" from point of impinge of the molten current, the solidification average *R* was calculated by:

$$R = \frac{t.v}{d} \quad \ldots\ldots\ldots\ldots\ldots\ldots \quad (1)$$

Where it is the thickness of the ribbon's and *v* is the wheel surface speed, R (the solidification average) is in the range of 10^{-5}_10^{-4} m/s. So from the observation, we noticed that solid ribbons which obtained depart the wheel surface after around a tenth of one roll where $d \approx 0.5$cm[15]. The samples prepared in this work are AL-Si_x (where x=1, 5, 9, and 13 in wt. %), weighted and put in a porcelain crucible to melt down at melt temperature of 750°C

Table 1: chemical compositions of starting materials (wt.%)

Alloy	Al wt.%	Si wt.%
Al	100	-
Al-Si	99	1
Al-Si	95	5
Al-Si	91	9
Al-Si	87	13

The parameters of this operation as the expulsion temperature and the linear speed of the copper wheel were limited at 31.4 m/s of the melt_spinning technique[16]. The flow rate is shown experimentally to be a significant melt_spun technique changing and depend on amenable instrument parameters which written by Liebermann. The parameter is studied by:

$$Q_f = V_r W t \quad \text{..... (2)}$$

Where (W) is the width of the ribbon (V_r) is the speed's ribbon and we can calculate (t) the average thickness by:

$$t = \frac{m}{lw\rho} \quad \text{..... (3)}$$

Where (m) is the mass of the ribbon, (l) is the length of the ribbon, (ρ) is the density_ray diffraction inspection was achieved on a Shimadzu (x_ray diffractometer(XRD) _30), employing Cu kα radiation (λ=1.5406 Å)via Ni_refinery. The microstructure inspect was performed on a scanning electron microscope (SEM) of type JSM_6510 LV JEOL (Japan), working at (30 kV) resolution in high vacuum mode, and 3.0 nm. The Vickers micro hardness examiner of type FM_7, Japan, enforcing a load of 25.0-gram force for 5.0,20.0,40.0,60.0,80.0 and 99.0 sec, via a diamond pyramid

3. Results and Discussions

3.1. Structure (x-ray diffraction analysis)

Structural characterization of melt_spun ALSi alloys are shown in Fig.2. shows the x_ray diffraction spectra from the ALSi (x=0,0.1,0.5,0.9 and 1.3wt.%) alloys produced by melt _spinning technique at a wheel speed $30.4\ m.sec^{-1}$ and ejection temperature of 1050 k. From all the x_ray diffraction examination, it was analyzed that the rapidly solidified ALSi alloy consists of supersaturated face_centered cubic α_Al and Si phases, except AL1 wt. %Si alloy where revealed that one phase α_Al which means that Si completely soluble in Al matrix. from x-ray pattern and by using Scherer's equation the lattice particle size can be calculated:

$$D_{hkl} = 0.891\lambda/\beta_{hkl}\cos\theta. \quad \text{..... (4)}$$

Where λ represents to wave length of Cu Kα=1.54056 A° β is the broadening of the full-width high maximum (FWHM), and θ is the reflection angle.

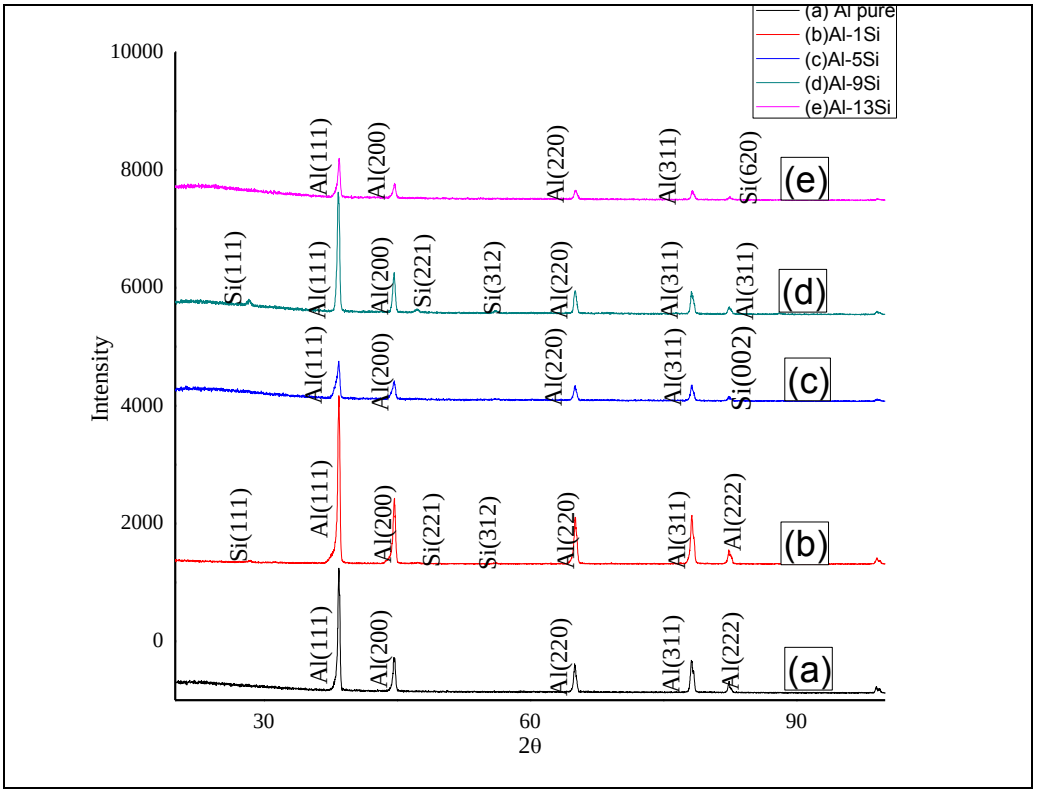

Fig.2. The XRD pattern of Al-Si melt-spun ribbons.

System wt.%	Phases observed	Crystal system	crystallite (nm)	Size	Lattice parameter (a) (A°)	Cell volume $(A^{\circ})^3$	Number of atoms/ unit cell
Al pure	α –Al	f.c.c	42.188		4.051	66.522	3.712
Al-0.1Si	Al	f.c.c	36.899		4.397	85.026	2.612
	Si	diamond cubic					
Al-0.5Si	Al	f.c.c	55.606		3.667	49.325	2.131
	Si	diamond cubic					
Al-0.9Si	Al	f.c.c	28.651		3.946	61.458	3.408
	Si	diamond cubic					
Al-1.3Si	Al	f.c.c	52.747		4.221	75.212	3.468
	Si	diamond cubic					

Table 2: phases observed, crystal system Number of atoms per unit cell, unit cell volume, lattice parameters, and crystallite Size of melt_spun alloys system.

3.2. Microstructure (Metallographic examination)

The Scanning electron microscope (SEM) micrograph detected a fine_grained structure for samples that prepared via melt spinning technique. the microstructure of Al_pure and Al–xSi (x=1, 5, 9 and 13 in wt.%)are showed in Fig.3.the observations showed that the Cge in Silicon content has a noticed effect on the system microstructure. We see the increase of Si content, making an increase of the particle size due to reducing the grain size and rising the mechanical characteristics as X_ray calculations showed. The microstructure shown in Fig. 3, t is observed that the primary -aluminum grains are present in the structure of Al-Si hypoeutectic in primary alpha solid solution of aluminum. The little amount of silicon can also be seen in the boundary region.

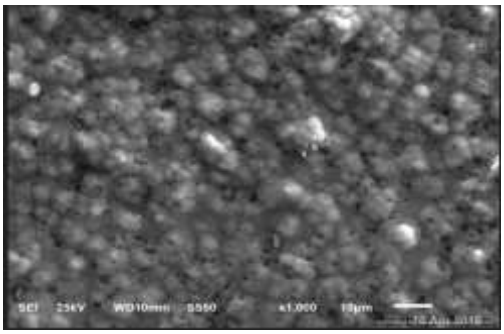

(a)Al pure

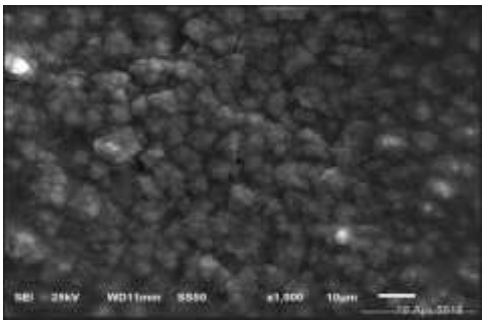

(b)Al-0.1 wt.%Si

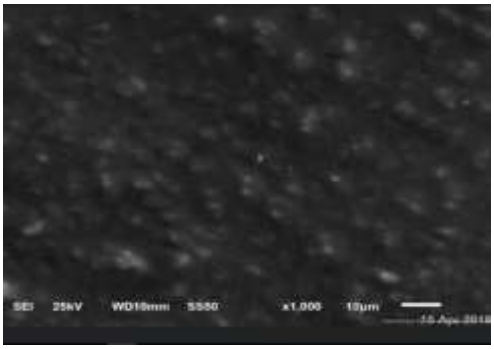

(c)Al-0.5 wt.% Si

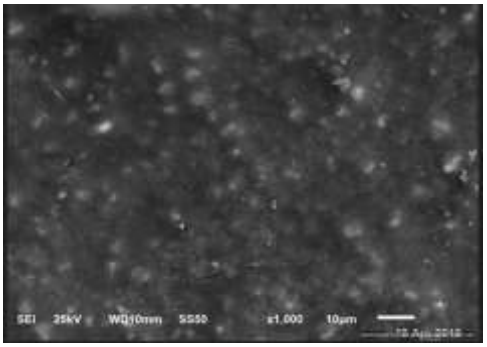

(d)Al-0.9 wt.% Si

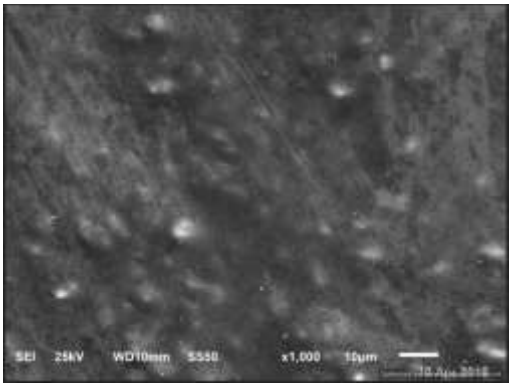

(e)Al-1.3 wt.% Si

Fig.3: (a, b, c, d, and e) SEM micrograph of melt-spun ribbon alloys.

4. Mechanical properties

4.1. Young's modulus, Internal friction, and thermal diffusivity

In Table 2, dynamic Young's modulus verity with content of silicon. It observed a raising of the young's modulus reach to the76 MPa at 1.3 wt.% Si. This observation is a result of elastic modulus with Silicon content can be studied in atomic bonding between Silicon and Aluminum result from rapid solidified. We observed that Young's modulus(E)has an increasing when the lattice constant (a) increase. The increase in (a) means the stretching of the Cell volume, the shape of the unit cell of the Al matrix is modified it may result in an increase in Young's modulus.

The internal friction (Q^{-1}) values is consider one of important features where it is indirect related to its elastic characteristics and can be calculated from resonance peak. During free vibration, and calculating the decay of vibration amplitude measurement, we can define the free vibration and the internal friction by:

$$Q^{-1} = 0.5773 \frac{\Delta f}{f_0} \quad \text{..... (5)}$$

The Values of internal friction Q^{-1} and Young Modulus E result of Al and Al-Six (where x=0.1, 0.5,0.9, and 1.3 wt.) alloys rapidly solidified from melt_spun ribbons restricted in table3.

Table 3: Mechanical properties of melt _ spun alloys.

Composition wt.% as melt spun Ribbons	Young's modulus (E) GPA	Bulk modulus (B) GPA	Shear modulus (G) GPA	Internal frication $\boldsymbol{Q^{-1}(10^{-3})}$
Al pure	66.81	73.12	24.4	45
Al-0.1Si	76.67	83.08	28.1	16
Al-0.5Si	62.08	65.09	23.2	19
Al-0.9Si	65.68	65.08	24.3	11
Al-1.3Si	76.30	73.04	28.8	26

Thermal diffusivity values of any material can be determined by The change of time rate of temperature determines the values when heat via through the material as restricted in table 3. Via reverberation frequency(f_o) where the top of damping happens using the dynamic reverberation technique, thermal diffusivity Can be calculated wher:

$$D_{th} = \frac{2d^2 f_\circ}{\pi} \quad \text{..... (6)}$$

At which, (*d*) is represented as the ribbon's thickness for Al_ pure and Al_Six (where x= 1, 5, 9 and 13 wt. %), melt_spun samples, we noticed that the thermal diffusivity has a higher value in Al_1Si sample than Al_ pure and Al_Si_x (where x= 5, 9 and 1 3 wt. %) alloys. However, there is a slight reduce of thermal diffusivity in Al_9Si sample, this is probably because of segregation.

Table 4: Thermal Diffusivity of melt_spun alloys.

Composition w.t% as melt spun Ribbons	Thermal Diffusivity $D_{th}10^{-3}(cm^2/sec)$
Al pure	9.5
Al-0.1Si	11.5
Al-0.5Si	7.59
Al-0.9Si	8.56
Al-1.3Si	10.47

4.2. Electrical resistivity of Al-Si alloys

by micro-ohmmeter equipment (BS 407) Resistivity can be measured with high accuracy from 1μΩ to 10KΩ to the selected specimens of Al-Si alloys. The specimens are obtained were registered to a unified shape to make sure the reproducibility of the measurement. In metals, the resistivity depends on the structural indefectibility of materials and particular elements purity. By negligible amount of impurities, It can be changed significantly. comparing of literature data [13,21]with our own measurements of resistivity, The electrical resistivity (ρ) of alloys at room temperature is measured and the results are explained in Fig 4. The resistivity decreases with raising Si concentration and the highest value was restricted of about $1.12x10^{-7}$Ωcm.

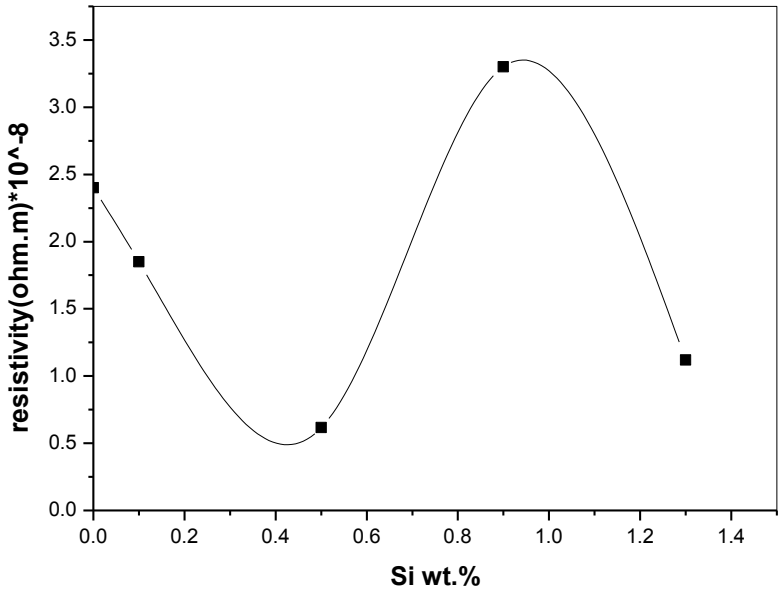

Fig 4: Electrical resistivity of melt-spun Al-Si alloys at room temperature with Si content.

4.3. Micro hardness test

By Vickers micro hardness, we can study the mechanical properties of Al_pure and Al-Six (where x=0.1,0.5,0.9 and 1.3 wt. %), melt_spun alloys, applying the standard Vickers equation, depending on literature of previous studies.

$$Hv = 2F\frac{\sin 68}{d^2} = 1.854\frac{F}{d^2} \quad \ldots\ldots\ldots\ldots\ldots\ldots \quad (7)$$

In which, H_V represents Vickers hardness, *d* is the average length diagonally, *F* represent the force of indentation or Load indent in 10 gram of force (gf) and via a constant geometric factor 1.854 is for the diamond pyramid. Figure 4 shows the variation of micro hardness H_v with Silicon content at 5sec. The increasing Silicon content, increase hardness number up to 881.02 MPa at 13 wt.% Si. There is an increase in hardness number because of the presence of solid solubility of Silicon in Aluminum matrix and the effect of rapid solidification.

4.4. Micro-creep

Figure 6. displays the relation between H_v versus time indent. It showed a decreasing of H_v varying time. The number of hardness can calculated by H_v=0.102F/S MPa [18]in which F represent the applied force in N, and S is the indentation surface area in mm^2. when the applied load is stable at 0.098 N, the hardness decreases because of indentation area increase. Increasing of area (strain) here is like the fractional change in area and, it can obtained by Strain (ε) =ΔS/S_0 [19], in which (ΔS) is the increase of surface area and (S_0) represent to the original area that measured at the lowest of the indentation time. The creep measurement by this technique is called" micro_creep" this expression of micro-creep attributed to enforcing the stress on a very small area compared to grain area, and it is observed by microscope. The relation between strain and indent time are showed in Figure 6, a typical creep curve is obtained. It showed that creep resistance of Al-13Si sample is higher than that of other samples. At first stage, the results registered a rapid increase of strain with the indent time starts from beginning up to 40 sec. of indentation time, and in the second stage, there is a slightly increase region where the strain rises by lower rates for all alloys. the hypereutectic Al-13Si alloy is consider the better creep resistance result of the other alloys as shown in Fig.6. this is due to the effect of solid solution and precipitation of Silicon in the Aluminum matrix. We can elucidate that The creep resistance increased as increasing Silicon concentration of the alloys

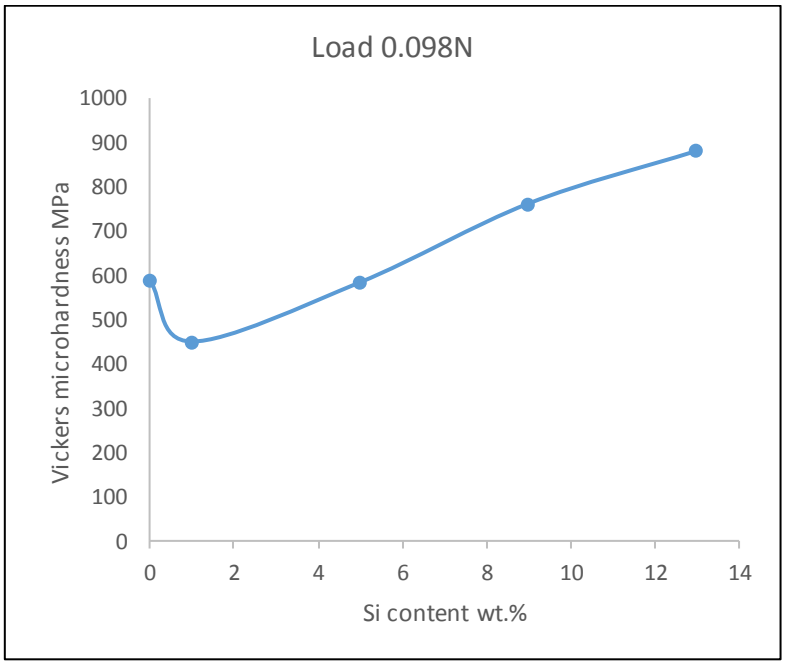

Fig. 5 The variation of Vickers micro hardness (H_v) with Silicon content.

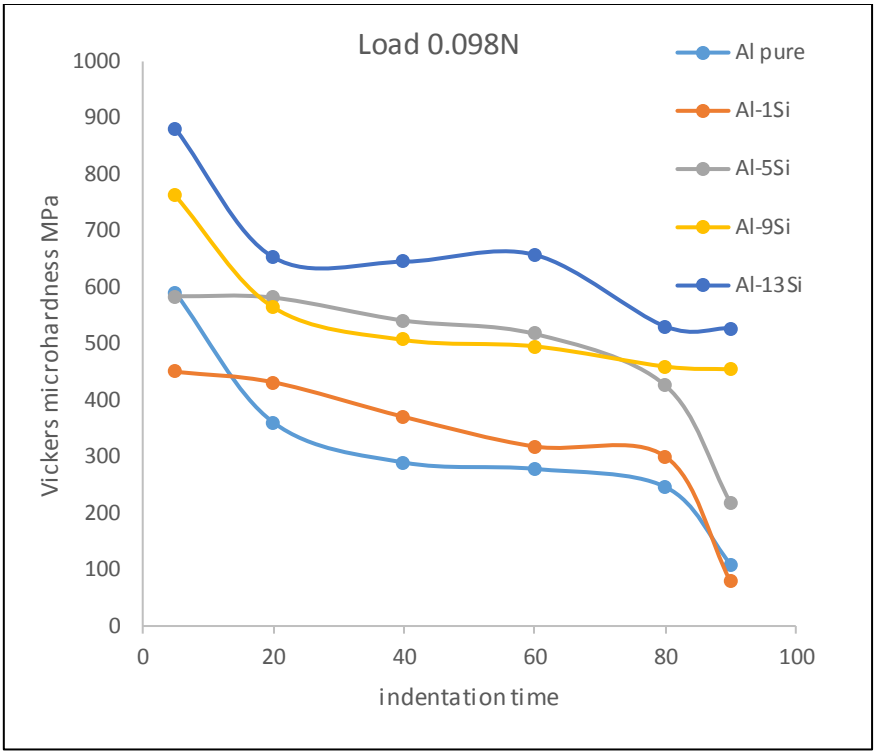

Fig. 6 Variation of Vickers micro hardness with indentation time of Al_Si alloys.

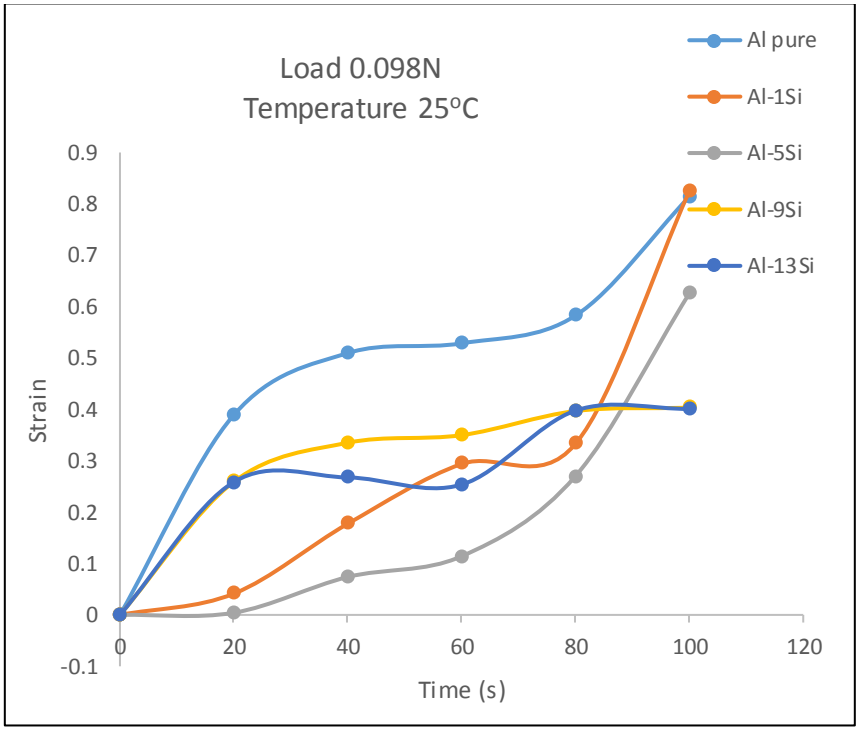

Fig. 7. The creep behavior of melt_spun of Al-Si alloys

It observed that at increasing loading time, the indentation length increase. Also, it's observed that the indentation length increases with the apply time. Substances that has a finer grain size, its indentation creep more readily as compared to the coarser-grained material. The values obtained of stress exponent (n) are 2.47, 1.65, 3.17, 8.9 and 11.28 for Al pure and Al-Six (where x= 0.1,0.5,0.9 and 1.3) (all in wt. %), the calculated values are given in Table 5, It is reported that limited stress range the indentation creep information can be explained

by a fixed stress exponent, example, the stress exponent raises with the increase of net section stress respectively. Juhasz et al [20], can obtain the stress exponent (n) by designing a tests on a superplastic lead_tin alloy utilizing Vickers hardness tests in steady_state creep with the following formula:

$$n = \left[\frac{\partial \ln d^*}{\partial \ln H_V}\right]_d \quad \ldots\ldots\ldots\ldots\ldots\ldots \quad (8)$$

Where d* is the rate of variation in indentation length, H_V represents to the number of Vickers hardness and d represents to the indentation diagonal length. This indicated to we will obtain a straight line if d is plotted against H_V on a double logarithmic scale, the slope of which is the stress exponents which shown in Fig. 8.

Table 5: the hardness number and stress exponent of melt_spun alloys system.

Alloy	Hv (MPa)	stress exponent (n)
Al pure	312.538	2.47
Al-0.1Si	324.951	1.652
Al-0.5Si	478.158	3.172
Al-0.9Si	540.47	8.9
Al-1.3Si	649.25	11.286

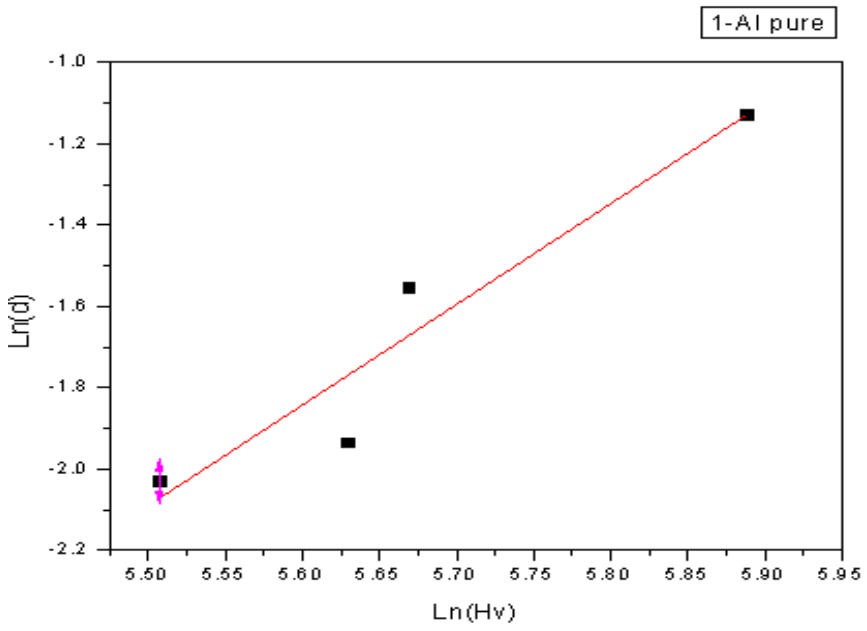

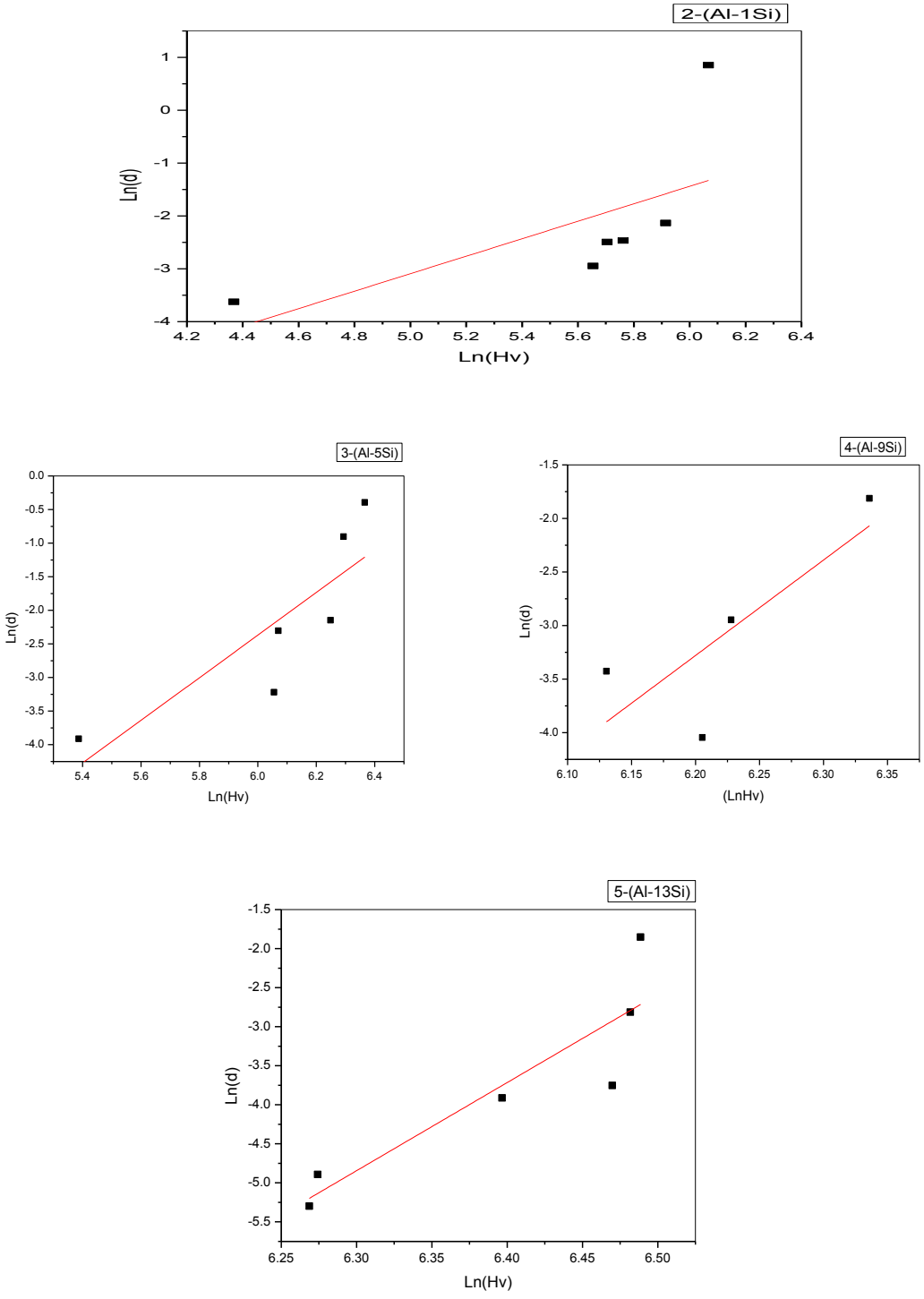

Fig.8. Indentation creep of melt_spun alloys.

Conclusions

The following conclusions were obtained as a result that the structural studies and mechanical performance of Al-Si based alloys were carried out using a single_roller melt spinning technique. The unusual properties exhibited by rapidly solidified metallic materials, produced by melt-spun single roller technique have led to technologically important developments in the design and production of a new generation of metastable intermediate phase-based up on aluminum.

1- Rapid solidification processing has been able to improve the internal friction and Young's modulus for the Al-containing Si.

2- RSP from the melt leads to formation of a α-Al and Si phases

3- The combination of mechanical strength and low internal friction with high corrosion resistance of melt-spun Al alloys may be exploited in a moving part of some machines. These are very useful to the proper working machine.

References

1. S.P. Nikanorov, M.P. Volkov, V.N. Gurin, Y.A. Burenkov, L.I. Derkachenko, B.K. Kardashev, L.L. Regel, W.R. Wilcox, Structural and mechanical properties of Al-Si alloys obtained by fast cooling of a levitated melt, 390 (2005) 63–69.

2. J.A. Lee, Cast Aluminum alloy for high-temperature applications(A) (B), 1 (2019)713-13.

3. W.R. Osório, N. Cheung, L.C. Peixoto, A. Garcia, Corrosion Resistance and Mechanical Properties of an Al 9wt % Si Alloy Treated by Laser Surface Remelting, 4 (2009) 820–831.

4. H. Kaya, M. Gu, H. Kaya, M. Gu, Dendritic Growth in an Aluminum-Silicon Alloy, 16 (2007) 12–21.

5. M.G. Kalhapure, P.M. Dighe, Impact of Silicon Content on Mechanical Properties of Aluminum Alloys, 4 (2015) 2013–2015.

6. F. Alshmri, Rapid Solidification Processing : Melt Spinning of Al-High Si Alloys, 390 (2012) 5–12.

7. B.V.S. Rao, A.C. Reddy, Fluidity of modified and unmodified Al-Si alloys in alumina investment shell moulds, Natl. Conf. Adv. Des. Approaches Prod. Technol. 4 (2005) 22–23.

8. S. Priyadarshini, S. Pattnaik, M.K. Sutar, Advancement in Property Improvement in Aluminium-Silicon Alloys : A Review, Int. J. Eng. Technol. Sci. Res. 4 (2017) 826–832.

9. L. Kloc, S. Spigarelli, E. Cerri, E. Evangelista, T. Langdon, An evaluation of the creep properties of two Al-Si alloys produced by rapid solidification processing, Metall. Mater. Trans. A. 27 (1996) 3871–3879.

10. O. Uzun, T. Karaaslan, M. Gogebakan, M. Keskin, Hardness and microstructural characteristics of rapidly solidified Al-8-16 wt.%Si alloys, J. Alloys Compd. 376 (2004) 149–157.

11. .L. Murray and A.J. McAlister, Bull. Alloy Phase Diagrams, 5.1, Feb.(1984)74-684.

12. T.J. Phys, Production and Structure of Rapidly Solidified Al-Si, J. Phys. 25 (2001) 455–466.

13. Yifan Sun,etal, ThermalandElectricalConductivityofLiquidAl–SiAlloys SpringerScience+BusinessMedia ,LLC,part of SpringerNature,40(2019)40-31.

14. Mustafa Kamal, AM Shaban, M El-Kady, Rizk Shalaby, Irradiation, mechanical and structural behaviour of Al-Zn-based alloys rapidly quenched from melt, Taylor & Francis Group (1996) 307-318.

15. M Kamal, AM Shaban, M El-Kady, RM Shalaby, Determination of structure-property of rapidly quenched aluminum-based bearing alloys before and after gamma irradiation , 2nd International Conference of Engineering Physics and Mathematics, Faculty of Engineering, Cairo University, Cairo (1994) 107-121.

16. H.H. Liebermann, The dependence of the Geometry of glassy alloy ribbons on the chill block melt-

spinning process parameters, Mater. Sci. Eng. 43 (1980) 203–210.

17. B.D. Cullity, Elements of X-ray Diffraction, 2nd edition, Addison-Wesley, 1978, p. 248.

18. Rizk Mostafa Shalaby, T. El-Ashram, Effect of rapid solidification and small additions of Zn and Bi on the structure and properties of Sn-Cu eutectic alloy, J. Electron. Mater. 34 (2005) 212–215.

19. Rizk Mostafa Shalaby, Effect of indium content and rapid solidification on microhardness and micro-creep of Sn-Zn eutectic lead-free solder alloy, 432 (2010) 427–432.

20. G. Physics, L. Estv, Investigation of the superplasticity of tin-lead eutectic by impression creep tests, 21 (1986) 3287–3291.

21. B. Kucharska∗ and J. Kowalczyk, Resistance Properties of Al-Si Coatings. 129 (2016) 18-23.